Glycobiology vol. 0 no. 0 pp. 1–9, 2011
doi:10.1093/glycob/cwr173
Advance Access publication on Month 00, 0000

Structural features for α-galactomannan binding to galectin-1

Michelle C Miller[2], Anatole A Klyosov[3], and Kevin H Mayo[1,2]

[2]Department of Biochemistry, Molecular Biology and Biophysics, University of Minnesota Health Sciences Center, 6-155 Jackson Hall, 321 Church Street, Minneapolis, MN 55455, USA and [3]Galectin Therapeutics Inc., 7 Wells Ave., Newton, MA 02459, USA

Received on September 13, 2011; revised on November 4, 2011; accepted on November 20, 2011

Galectins have a highly conserved carbohydrate-binding domain to which a variety of galactose-containing saccharides, both β- and α-galactosides, can interact with varying degrees of affinity. Recently, we demonstrated that the relatively large α(1 → 6)-D-galacto-β(1 → 4)-D-mannan (Davanat) binds galectin-1 (gal-1) primarily at an alternative carbohydrate-binding domain. Here, we used a series of α-galactomannans (GMs) that vary in their mannose-to-galactose ratios for insight into an optimal structural signature for GM binding to gal-1. Heteronuclear single-quantum coherence nuclear magnetic resonance spectroscopy with ^{15}N-labeled gal-1 and statistical modeling suggest that the optimal signature consists of α-D-galactopyranosyl doublets surrounded by regions of about four or more "naked" mannose residues. These relatively large and complex GMs all appear to interact with varying degrees at essentially the same binding surface on gal-1 that includes the Davanat alternative binding site and elements of the canonical β-galactoside-binding region. The use of two small, well-defined GMs [6^1-α(1 → 6)-D-galactosyl-β-D-mannotriaose and 6^3,6^4-di-α(1 → 6)-D-galactosyl-β-D-mannopentaose] helped characterize how GMs, in general, interact in part with the canonical site. Overall, our findings contribute to better understanding interactions of gal-1 with larger, complex polysaccharides and to the development of GM-based therapeutics for clinical use.

Keywords: galactose / glycan / lectin / NMR / protein

Introduction

Galectins, which are generally known to bind to β-galactosides at a canonical site in the carbohydrate recognition domain (Barondes et al. 1994), exhibit various extracellular activities to mediate cell–cell and cell–matrix adhesion and migration by interacting with various glycan groups of cell surface glycoconjugates (Liu and Rabinovich 2005). Galectin-1 (gal-1), for example, interacts with various glycoconjugates of the extracellular matrix (e.g. laminin, fibronectin, β1 subunit of integrins, ganglioside GM1 and lysosomal membrane-associated proteins lamp 1 and 2), as well as those on endothelial cells (Neri and Bicknell 2005; e.g. integrins $\alpha_v\beta_3$ and $\alpha_v\beta_5$, ROBO4, CD36 and CD13) and on T lymphocytes (e.g. CD7, CD43 and CD45) where it is known to induce apoptosis (Perillo et al. 1995, 1997). Their binding to cell surface glycoproteins can also trigger intracellular activity, e.g. elements of the Ras-MEK-ERK pathway (Fischer et al. 2005).

The β(1 → 4)-galactoside lactose (Gal-β(1 → 4)-Glc) is one of the simplest carbohydrates with which galectins interact in vitro (Barondes et al. 1994), and structural knowledge of saccharide–galectin interactions has generally been limited to studies with such simple saccharides (Nesmelova, Dings, et al. 2008). However, glycans in situ are larger, heterogeneous in size and composition and densely packed, and it is likely that gal-1 in vivo interacts to some extent with various other saccharide units. Although β-D-galactose units comprise 23% of all terminal monosaccharides in mammalian cell surface glycans, α-D-galactose and D-mannose (in various anomeric states) comprise ~2.3 and 18.9% of them, respectively (Werz et al. 2007). We recently reported that an α-galactomannan (GM), Davanat, derived from *Cyamopsis tetragonoloba* (guar gum) indeed interacts with gal-1 and over a relatively large surface area that is located primarily on that face of the protein opposite to its canonical lactose-binding site (Miller, Klyosov, Mayo, et al. 2009).

Davanat is currently being used against metastatic colorectal cancer in phase II clinical trials (http://clinicaltrials.gov/ct2/show/NCT00110721) and has been proposed as an antagonist of gal-1 which is known to play a crucial role in the adhesion and migration of highly proliferative endothelial cells in tumors (Rabinovich 2005; Thijssen et al. 2006). The observation that gal-1 apparently is not involved in normal bodily processes, like wound healing (Cao et al. 2002), suggests that the increased expression of gal-1 found in tumors (Thijssen et al. 2006) renders the protein an excellent target for therapeutic purposes. A better understanding of the structural features of GMs, like Davanat, that promote interactions with galectins would be quite useful to the development of other GM-based anticancer agents.

[1]To whom correspondence should be addressed: Tel: +1 612 625 9968; Fax: +1 612 625 2163; e-mail: mayox001@umn.edu

composed of an α(1 → 6)-mannan backbone and variously linked α(1 → 2) and α(1 → 3) mannose residues. Nevertheless, both mannans interact to essentially the same degree, albeit minimally, with gal-1.

In all cases, the differential change in gal-1 resonance intensity is primarily due to exchange between/among gal-1 and binding sites on these GMs that occurs on the intermediate chemical shift time-scale (Keeler 2005). HSQC data also indicate that the overall folded structure of gal-1 is not significantly perturbed by GM or mannan binding, because chemical shifts of resonances remaining during the titration are mostly unchanged. Because GM-gal-1-binding events fall in the intermediate exchange regime, Figure 2 shows examples of two HSQC resonance broadening maps (Miller, Klyosov, Mayo, et al. 2009) for GM 1.8 and GM 2. Here, we show differential broadening at a molar ratio of each of these GMs where most resonances are still observed, but are at lower intensities due to apparent broadening. The interpretation of HSQC broadening maps is essentially the same as with HSQC chemical shift mapping (Rajagopal et al. 1997), i.e. those resonances that are broadened the most are associated with that site(s) of glycan interaction on gal-1. Fractional changes are calculated by subtracting from 1 the intensity of a given HSQC cross-peak divided by that in pure gal-1 at the same protein concentration. A value of 1 indicates that a resonance is no longer apparent, and a value of zero indicates no change in resonance intensity.

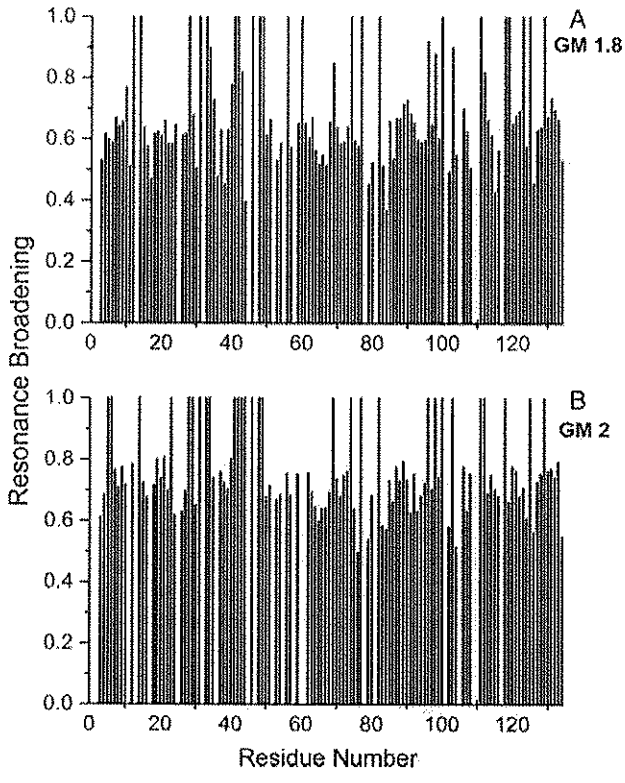

Fig. 2. HSQC resonance broadening maps are shown for GM binding to gal-1. Fractional changes in gal-1 resonance intensities observed for gal-1 in the presence of GMs are exemplified with resonance broadening maps for GM 1.8 (3 mg/mL, **A**) and GM 2 (1.8 mg/mL, **B**) vs the amino acid sequence of gal-1. Data are shown under conditions where most gal-1 resonances are still apparent. A value of 1 indicates that the resonance associated with that particular residue is no longer apparent, and a value of zero indicates no change in resonance intensity.

Since resonances in the intermediate exchange regime are initially chemically shifted as they are broadened (some more than others), we also show HSQC chemical shift maps (Rajagopal et al. 1997) for some of these GMs in Figure 3. Resonances that are highly broadened prior to significant shift changes, of course, are absent from these plots, and for some others that may not be readily apparent in HSQC data shown, cross-peaks could be followed in by going more into the spectral floor of the contour plots. Correlation plots of the chemical shift difference, $\Delta\delta$, for one GM vs another all give correlation coefficients in the range 0.6–0.72, suggesting similar modes of interaction with gal-1.

Both broadening and chemical shift mapping (Figures 2 and 3) provide a fairly consistent picture as to where these GMs interact on gal-1. Although there could be multiple modes of interaction, it appears that the GMs interact primarily with the same region on gal-1, as illustrated in Figure 4. Gal-1 has a β-sandwich structure that is comprised of 11 β-strands, with the lactose-binding site primarily comprising β-strands 4, 5, 6 and 9, and the dimer interface is made up of strands 1 and 11. The proposed primary site for interaction is at the edge of the β-sandwich from the top of the canonical

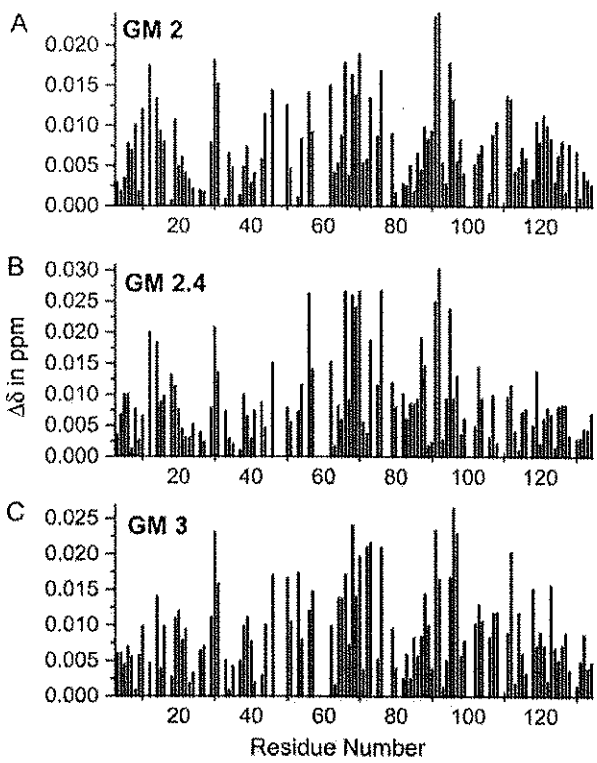

Fig. 3. HSQC chemical shift mapping is shown for GM binding to gal-1. ^{15}N- and ^{1}H-weighted chemical shift changes, $\Delta\delta$, between ^{15}N-gal-1 (the absence of ligands) and ^{15}N-gal-1 in the presence of near saturating concentrations of GM 2 (**A**), GM 2.4 (**B**) and GM 3 (**C**) are plotted vs the amino acid sequence of gal-1.

For example, a Man/Gal ratio of 1.0 indicates that there would be no isolated "clusters" of $(Gal/Man)_n$ or $(Man)_n$, and therefore $P = 0$ in either case. Alternatively, for a Man/Gal of 2.0, $P = 0.5^2 \times 0.5^n$. This formula also gives the probability of having doublets, triplets, quadruplets etc. of "naked" Man residues. If we take the "naked" Man residues to be 1.0 and Man/Gal = 2, $P(1-q) = 0.5^2 \times 0.5^1 = 0.125$ or 12.5%. For Man/Gal = 1.1, the average ratio of Gal/Man residues and "naked" Man residues would be 0.909:0.091, and the probability of having isolated Gal/Man singlets ($n = 1$), doublets ($n = 2$) etc. is given as $0.091^2 \times 0.909^n$. These probabilities would be the same for sequential $(Man)_n$ residues in the GM backbone.

We can achieve essentially the same result by randomly generating a probability distribution simply by "tossing a coin", e.g. 300 times, with tails for having (Man) and heads for having (Gal/Man) residues along the GM backbone. For $n = 1$ to $n = 6$, we can calculate percentages from these probabilities as 13.3 ± 2.1, 6.3 ± 1.4, 3.0 ± 1.0, 1.6 ± 0.7, 0.7 ± 0.5 and 0.3 ± 0.3%, respectively. This indicates that for Man/Gal = 2, the above formulae adequately describe the distribution of (Gal/Man) and (Man) residues along the GM backbone.

Figure 6A plots $P(n)$ vs the Man/Gal ratio for $n = 1$ to $n = 6$. Three observations can be made: (i) the $P(n)$ maximum shifts from a Man/Gal ratio of ~3 at $n = 1$ to ~1.3 at $n = 6$; (ii) at lower Man/Gal ratios, the increase in $P(n)$ to its maximum becomes greater as the n value is decreased and (iii) at higher Man/Gal ratios, the decrease in $P(n)$ from its maximum becomes greater as the n value is increased. To compare these trends with experiment, Figure 6B plots changes in gal-1 HSQC resonance broadening averaged over all residues vs the Man/Gal ratio for data acquired at GM concentrations from 0.2 to 3 mg/mL. Increased broadening is proportional to increased avidity of gal-1 for these GMs. At any GM concentration, broadening is greatest for GM 2 (a Man/Gal ratio of 2) and decreases on either side of this Man/Gal ratio. The probability distribution for $n = 2$ (Figure 6A) is most consistent with these experimental data in that $P(n)$ max occurs at about a Man/Gal ratio of 2. For $n = 1$, $P(n)$ max is around 3, and for $n = 3$, $P(n)$ max is around 1.6 or 1.7. Furthermore, for $n = 2$, $P(n)$ falls ~35% from its maximum by the Man/Gal ratio of 4, and this is about the same percentage decrease observed experimentally (Figure 6B). Over the same range, $P(n)$ falls at most by 10% for $n = 1$ and by ~70% for $n = 3$, and greater as the n value is increased further.

This simple model, which is consistent with our experimental data, strongly suggests that the structural signature for binding of gal-1 to GMs is the presence of α-D-galactopyranosyl doublets, randomly distributed over the GM backbone and interspersed with regions of "naked" mannose.

Binding of gal-1 to a mannotriaose and mannopentaose

We next investigated whether, and if so how, gal-1 binds the α-D-galactopyranosyl doublet signature in the context of a simple mannopentaose [6^3,6^4-di-α(1 → 6)-D-galactosyl-β-D-mannopentaose], with a mannotriaose [6^1-α(1 → 6)-D-galactosyl-β-D-mannotriaose] and lactose as controls. For this, we performed the same ^{15}N-gal-1 HSQC titrations using these simple saccharides. Figure 7A and B shows HSQC expansions and spectral overlays through these titrations, and Figure 7C shows the same with lactose for comparison. From these data, it is apparent that both GM mannotriaose and mannopentaose, like lactose, interact with gal-1. Moreover, because gal-1 resonances are primarily chemically shifted (like lactose; Miller, Nesmelova, et al. 2009) and are not highly broadened, intrinsic-binding affinity is relatively weak vis-à-vis binding avidity of gal-1 to the larger and more complex GMs. Inserts in Figure 7A–C plot the average chemical shift changes for the top 30 shifting residues vs the saccharide concentration, respectively. From the mid-points of these curves, we can estimate apparent K_d values of $\sim 21 \times 10^{-3}$ and $\sim 6 \times 10^{-3}$ M for the GM mannotriaose and GM mannopentaose, respectively, compared with that of $\sim 0.3 \times 10^{-3}$ M for lactose. As expected, both GM mannotriaose and mannopentaose bind gal-1 with much lower affinities than does lactose.

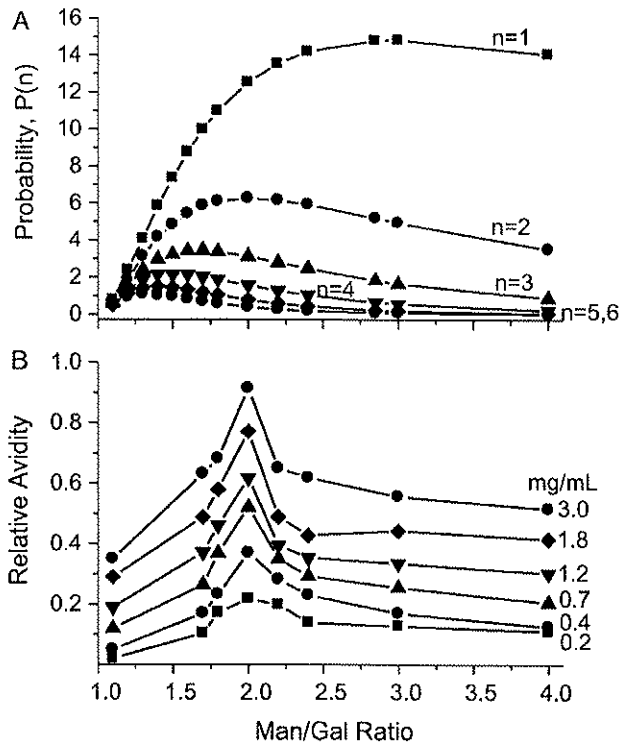

Fig. 6. (**A**) Probabilities (relative distributions) $P(n)$ of isolated sequences $(Gal/Man)_n$ for n between 1 and 6 along the galactomannan backbone. "Isolated" in this context means surrounded by "naked" (unsubstituted) single or multiple (Man) residues. Only one Gal residue can be attached to one Man residue, forming a (Gal/Man) pair. A random distribution of Gal residues along the galactomannan backbone, hence, a random distribution of $(Gal/Man)_n$ combinations ($n = 1$–6) is assumed for these calculations. This random distribution is described by formula $P = q^2 \times (1-q)^n$, where q is a fraction of "naked" Man residues in the galactomannan, and $(1-q)$ is a fraction of Gal/Man pairs in the galactomannan. (**B**) The effect of 1,4-β-D-galactomannans (GMs) with different degrees of attachment of (1 → 6)-α-D-Gal residues to (1 → 4)-β-D-Man residues in the GM backbone, described as the (Man/Gal) ratio, on the binding avidity of these GMs to gal-1. Binding avidity here is defined as the average broadening of ^{15}N-gal-1 HSQC spectral peaks upon the interaction with these GMs.

In both cases, gal-1 sequences that show the greatest differences include residues 29–32, 48–76, 90–92 and 100/104. Residues within the 48–76 sequence (β-strands 4 and 5, along with turn 51–54 and loop 65–76) essentially form the canonical lactose-binding site. For example, R48, N61 and E71 form hydrogen bonds with groups from lactose and W68 interacts directly with the galactose ring of lactose via CH–π stacking interactions (Nesmelova et al. 2010). Differences in residues 29–32 in the loop going into β-strand 3 are essentially explained by proximity to R48–F49. There are also significant differences with residues 87/90–92 and 100 which lie on the opposite side of the β-sandwich. Internal β-sandwich residue L100, for example, interacts directly with I58, which likely explains this difference. However, it is unclear why residues 90–92 are so affected, because they are relatively distant from the lactose-binding domain, other than to say that they are highly perturbed by saccharide binding. Overall, the GM mannopentaose has greater effects at R48/L32, I58, T70, E71, E74 and V76. This is interesting because GM mannopentaose binding to gal-1 is much weaker than with lactose, and the larger mannopentaose appears to exhibit greater interactions particularly at the 70–76 loop which lies at the top of the lactose-binding domain. This region then flows to the side of the β-sandwich with which the larger GMs interact, as discussed in the previous sections.

Discussion

Using a series of GMs with different Man/Gal ratios, we report here on the structural signature for optimal binding of GMs to gal-1. One feature of this signature is the presence of α-D-galactopyranosyl doublets, randomly distributed over the GM backbone. This is based on the experimental observations of HSQC resonance broadening, which indicates that gal-1 has the strongest interactions with a GM having a Man/Gal ratio of 2, and much less so with GMs having either smaller or larger Man/Gal ratios. This conclusion is supported by statistical analyses using a simple model that is parameterized for the fraction of Gal/Man clusters, the fraction of "naked" Man residues and the number of sequential Gal/Man residues surrounded by "naked" Man residues. The most acceptable probability distribution is for a Man/Gal ratio of 2, consistent with experimental observations. At Man/Gal ratios higher than 2, Gal residues would be more scattered along the mannopyranosyl polymer chain, with lower probability of having isolated clusters of Gal_n residues. At lower Man/Gal ratios approaching 1.0 (i.e. all Man residues would have attached Gal residues), the probability of having isolated Gal clusters, surrounded with "naked" Man residues, would also be low.

This investigation also suggested another facet to the optimal signature, namely that α-D-galactopyranosyl doublets should be flanked by regions of "naked" mannan. Doing this would provide less sterical hindrance for the α-D-galactopyranosyl doublet to interact with gal-1. This suggestion is supported by our experimental observation of relatively greater binding of gal-1 to GMs with Man/Gal ratios of 3 or 4 vis-à-vis GM with a Man/Gal ratio of 1.1, which has essentially no stretches of "naked" mannan. Binding still occurs, but to a lesser extent. Previous studies also demonstrated that gal-1 can bind to a polymannan, albeit more weakly than to a GM (Miller, Klyosov, Mayo, et al. 2009). Moreover, HSQC broadening mapping indicates that any of these GMs with different Man/Gal ratios interacts at least partly at an alternative site adjacent to the canonical lactose-binding domain and on the backside β-sheet of the gal-1 β-sandwich. This observation is also consistent with that reported earlier for polymannan interaction with gal-1 (Miller, Klyosov, Mayo, et al. 2009).

β-D-Mannanase hydrolysis studies of GMs with different Man/Gal ratios (like the GMs investigated here) do indicate that GMs with random distributions of Gal residues will contain significant segments of backbone mannose residues devoid of galactose moieties. Even though different β-D-mannanases exhibit different modes of GM hydrolysis (McCleary and Matheson 1983; McCleary et al. 1983, 1984), it is generally the case that GMs with Man/Gal ratios of ~2 and above will have segments of four or more "naked" mannans. For example, the *Aspergillus niger* β-D-mannanase digestion of several GMs with different Man/Gal ratios shows that the degree of hydrolysis is greatest when four or more "naked" mannans are present, presumably because of steric hindrance from galactose moieties in other regions (see Table 3 in McCleary and Matheson 1983). In another study, hydrolysis of three GMs (Man/Gal ratios of 1.7, 3.0 and 4.0) using two endo-β-mannanases (from *Chrysosporium lucknowense* and *Trichoderma reesei*) results in relative degrees of conversion of 1.0:3.3:4.4 and 1.0:3.3:3.3, respectively. Assuming that β-mannanase-catalyzed hydrolysis can occur at "naked" sequences of Man from $n=1$ to $n=6$, then the limited degrees of conversion for these Man/Gal ratios would be 0.6:0.8:1.0 which is quite different from what is observed experimentally, i.e. 3.3/4.4:3.3:1.0. Calculated probabilities for $n=1$ to $n=6$ indicate that these β-mannanases preferentially digest GMs at sites with four (or more) "naked" Man residues in the polymer backbone (personal communication from Prof. A.P. Synitsyn *et al.*, Department of Chemistry, Moscow State University, unpublished results).

Our NMR gal-1-binding studies with 6^1-α(1 → 6)-D-galactosyl-β-D-mannotriaose and $6^3,6^4$-di-α(1 → 6)-D-galactosyl-β-D-mannopentaose indicate that α-D-galactopyranosyl doublets of these two small GMs interact at the canonical lactose-binding region. Nevertheless, their interactions at that site are expectedly different from those of the β-galactoside, as are the induced indirect conformational effects resulting from binding. Compared with lactose, GM mannopentaose in particular shows greater effects on residues within the 70–76 loop which lies at the top of the lactose-binding domain. It is intriguing to propose that this is due to direct interactions of the GM mannopentaose with this loop, which is part of the site with which the larger GMs primarily have also been proposed to interact. Consequently, one possible structural model for how larger GMs interact with gal-1 is to have a segment with galactose moieties interact at the canonical lactose-binding site, while, for example, a segment of "naked" mannan folds over and interacts with the side of the β-sandwich, as illustrated in Figure 4.

Knowledge of this structural signature for GM binding to gal-1 is not only important to better understand galectin–

Acknowledgements

We are most grateful and indebted to Prof. Linda Baum and Mabel Pang of the Department of Pathology and Laboratory Medicine, UCLA for providing us with their expression system (vector/plasmid) for human gal-1.

Conflict of interest

None declared.

Abbreviations

gal-1, galectin-1; GM, α-galactomannan; HSQC, heteronuclear single quantum coherence; ^{15}N-gal-1, ^{15}N-enriched gal-1; NMR, nuclear magnetic resonance.

References

Barondes SH, Castronovo V, Cooper DN, Cummings RD, Drickamer K, Feizi T, Gitt MA, Hirabayashi J, Hughes C, Kasai K, et al. 1994. Galectins: A family of animal β-galactoside-binding lectins. *Cell*. 76:597–598.

Cao Z, Said N, Amin S, Wu HK, Bruce A, Garate M, Hsu DK, Kuwabara I, Liu FT, Panjwani N. 2002. Galectins-3 and -7, but not galectin-1, play a role in re-epithelialization of wounds. *J Biol Chem*. 277:42299–42305.

Daas PJH, Schols HA, de Jongh HHJ. 2000. On the galactosyl distribution of commercial galactomannans. *Carbohydr Res*. 329:609–619.

Delaglio F, Grzesiek S, Vuister GW, Zhu G, Pfeifer J, Bax A. 1995. *J Biomol NMR*. 6:277–293.

Fischer C, Sanchez-Ruderisch H, Welzel M. 2005. Galectin-1 interacts with the α5β1 fibronectin receptor to restrict carcinoma cell growth via induction of p21 and p27. *J Biol Chem*. 280:37266–37277.

Ilyina AV, Mestechkina NM, Shcherbukhin VD, Varlamov VP. 2006. Depolymerization of legume seed galactomannan by Celloviridin G20x. *Prikladnaya Biokhimiya I Mikrobiologiya*. 42:580–586.

Johnson BA, Blevins RA. 1994. *J Biomol NMR*. 4:603–614.

Keeler J. 2005. *Understanding NMR Spectroscopy*. New York: Wiley and Sons.

Liu FT, Rabinovich GA. 2005. Galectins as modulators of tumour progression. *Nat Rev Cancer*. 5:29–41.

Lopez-Lucendo MF, Solis D, Andre S, Hirabayashi J, Kasai K, Kaltner H, Gabius H-J, Romero A. 2004. Growth-regulatory human galectin-1: Crystallographic characterisation of the structural changes induced by single-site mutations and their impact on the thermodynamics of ligand binding. *J Mol Biol*. 343:957–970.

McCleary BV, Dea ICM, Windust J, Cooke D. 1984. Interaction properties of D-galactose-depleted Guar galactomannan samples. *Carbohydr Polymers*. 4:253–270.

McCleary BV, Matheson NK. 1983. Action patterns and substrate-binding requirements of β-D-mannanase with mannosaccharides and mannan-type polysaccharides. *Carbohydr Res*. 119:191–219.

McCleary BV, Nurthen E, Taravel FR, Joseleau J-P. 1983. Characterization of the oligosaccharides produced on hydrolysis of galactomannan with β-D-mannanase. *Carbohydr Res*. 118:91–109.

Mestechkina NM, Shcherbukhin VD. 1991. Galactomannan from *Galega orientalis* Lam. Seeds. *Appl Biochem Microbiol*. 26:648–651.

Miller MC, Klyosov AA, Mayo KH. 2009. The α-galactomannan Davanat binds galectin-1 at a site different from the conventional galectin carbohydrate binding domain. *Glycobiology*. 19:1034–1045.

Miller M, Klyosov A, Platt D, Mayo KH. 2009. Using pulse field gradient NMR diffusion measurements to define molecular weight distributions in glycan preparations. *Carbohydr Res*. 344:1205–1212.

Miller MC, Nesmelova IV, Platt D, Klyosov A, Mayo KH. 2009. Carbohydrate binding domain on galectin-1 is more extensive for a complex glycan than for simple saccharides: Implications for galectin-glycan interactions at the cell surface. *Biochem J*. 421:211–221.

Neri D, Bicknell R. 2005. Tumour vascular targeting. *Nat Rev Cancer*. 5:436–446.

Nesmelova IV, Dings RPM, Mayo KH. 2008. Understanding galectin structure-function relationship to design effective antagonists. In: Klyosov AA, Witczak ZJ, Platt D, editors. *Galectins*. Hoboken, NJ: John Wiley & Sons, pp. 33–69.

Nesmelova IV, Ermakova E, Daragan VA, Pang M, Menéndez M, Lagartera L, Solis D, Baum LG, Mayo KH. 2010. Lactose binding to galectin-1 modulates structural dynamics, increases conformational entropy, and occurs with apparent negative cooperativity. *J Mol Biol*. 397:1209–1230.

Nesmelova IV, Pang M, Baum LG, Mayo KH. 2008. ^{1}H, ^{13}C, and ^{15}N backbone and side-chain chemical shift assignments for the 29 kDa human galectin-1 protein dimer. *J NMR Assign*. 2:203–205.

Perillo NL, Pace KE, Seilhamer JJ, Baum LG. 1995. Apoptosis of T cells mediated by galectin-1. *Nature*. 378:736–739.

Perillo NL, Uittenbogaart CH, Nguyen JT, Baum LG. 1997. Galectin-1, an endogenous lectin produced by thymic epithelial cells, induces apoptosis of human thymocytes. *J Exp Med*. 185:1851–1858.

Platt D, Klyosov AA, Zomer E. 2006. In: Klyosov AA, Witczak ZJ, Platt D, editors. *Carbohydrate Drug Design*. ACS Symposium Series, 932. Washington (DC): American Chemical Society. pp. 49–66.

Rabinovich GA. 2005. Galectin-1 as a potential cancer target. *Br J Cancer*. 92:1188–1192.

Rajagopal P, Waygood EB, Reizer J, Saier MH, Klevit RE. 1997. Demonstration of protein–protein interaction specificity by NMR chemical shift mapping. *Protein Sci*. 6:2624–2627.

Shcherbukhin VD. 1992. Galactomannans from seeds of the leguminous plants. *Soviet Union Food Hydrocolloids*. 6:3–7.

Thijssen VL, Postel R, Brandwijk RJ, Dings RP, Nesmelova I, Satijn S, Verhofstad N, Nakabeppu Y, Baum LG, Bakkers J, et al. 2006. Galectin-1 is essential in tumor angiogenesis and is a target for antiangiogenesis therapy. *Proc Natl Acad Sci USA*. 103:15975–15980.

Werz DB, Ranzinger R, Herget S, Adibekian A, von der Lieth C-W, Seeberger PH. 2007. Exploring the structural diversity of mammalian carbohydrates ("glycospace") by statistical databank analysis. *Chem Biol*. 2:685–691.